J Mater Sci (2009) 44:4205–4209
DOI 10.1007/s10853-009-3568-7

LETTER

Ultrastructure characterization of hydroxyapatite nanoparticles synthesized by EDTA-assisted hydrothermal method

Renlong Xin · Kaifeng Yu

Received: 12 March 2009 / Accepted: 12 May 2009 / Published online: 28 May 2009

Introduction

Hydroxyapatite (HA, $Ca_{10}(PO_4)_6(OH)_2$) is similar to the inorganic phase of human bone, tooth dentin, and enamel in chemistry and structure. Thus, synthetic HA ceramic exhibits excellent bioactivity and biocompatibility, and can be used as bone graft substitutes and bone fillers. In the last decade, the synthesis and characterization of HA particles have attracted extensive interest of research [1–3], and considerable attention was focused on the syntheses of HA with controlled morphology, size and crystallinity because such parameters have strong impact on the in vivo performance of HA [4–13].

A variety of processing routes have been used to synthesize HA such as chemical precipitation, hydrothermal processing, microwave irradiation, microemulsion, plasma spraying, sputtering/ion beam deposition, laser ablation, electrodeposition, and electrophoretic deposition [5–7, 11, 13–25]. Among the several routes, hydrothermal route is one of the most investigated methods; it can prepare HA crystals with controlled size and shape by the use of surfactants, such as ethylenediamine tetraacetic acid (EDTA), and so on [4, 6, 18, 19]. However, although the preparation of HA particles by hydrothermal method have been widely reported, the orientation and ultrastructure of the prepared HA particles have been rarely studied [26]. Moreover, it is not clear whether HA particles were precipitated directly or by intermediate phases in hydrothermal conditions.

In this article, HA nanoparticles with the length of 50–150 nm were synthesized by hydrothermal method with EDTA surfactant. The orientation and ultrastructure of the as-synthesized nanoparticles were characterized by X-ray diffraction (XRD) and transmission electron microscopy (TEM). Octacalcium phosphate (OCP, $Ca_8H_2(PO_4)_6 \cdot 5H_2O$), one of the intermediate phases of HA was identified in the hydrothermally synthesized nanoparticles by high-resolution transmission electron microscopy (HRTEM).

Experimental

All the reagents were of analytical grade and used without further purification. In a typical procedure, 50 mL of a mixed solution of $Ca(NO_3)_2 \cdot 4H_2O$ (0.5 M) and EDTA (0.1 M) was first prepared and then added dropwise into 50 mL of Na_2HPO_4 (0.3 M) under intense stirring. The initial pH of the mixed solution of $Ca(NO_3)_2 \cdot 4H_2O$ and EDTA was measured to be 11.5. After mixing with Na_2HPO_4, the pH of the new mixed solution was adjusted to 9 by adding NaOH solution, and then, the mixed solution was magnetically stirred on a hotplate (60 °C) for 2 h. After that, the mixed solution was kept in Teflon flasks and sealed tightly for hydrothermal reactions. The flasks were hold in oven at 120 °C or 180 °C for 12 h. After hydrothermal processing, white HA precipitates were filtered, washed thoroughly with deionized water, and oven-dried at 50 °C for 24 h.

Crystal phase of the precipitates was determined by powder XRD using Cu Kα radiation (X'pert pro-MPD, PANalytical, the Netherlands). The samples were scanned

R. Xin (✉)
College of Materials Science and Engineering, Chongqing University, Sha Zheng Jie 174#, Sha Ping Ba District, Chongqing, China
e-mail: rlxin@cqu.edu.cn

K. Yu
China Key Laboratory of Automobile Materials of Ministry of Education & Department of Materials Science and Engineering, Jilin University, Changchun, China

in the 2θ range of 3–58°. The precipitates were ultrasonically dispersed in ethanol to form dilute suspensions, and then, a few droplets were put on copper grids coated with amorphous carbon film for further examination by TEM (JSM2010F, JEOL, Japan). The structure of individual precipitate was revealed by selected area electron diffraction (SAED) and HRTEM using an accelerating voltage of 200 kV.

Results and discussion

Calcium phosphate precipitates were produced by hydrothermal method in the presence of EDTA. Figure 1 shows the representative TEM images of the precipitates produced at different temperatures. It can be seen that the dominance of the precipitates exhibits plate-shaped or rod-like morphologies for the 120 °C and 180 °C samples. However, there is also a small portion of tiny crystals (less than 50 nm in size) with irregular shape. The size of the precipitates is in the range of 50–150 nm and the aspect ratio varies from 2 to 4. The contrast of the precipitates is very low in electron microscope indicating they have very small thickness. Thus, heretofore the precipitates are referred to be plate-shaped. In addition, Fig. 1 indicates that the temperature increase caused no significant changes on the morphology and size of the precipitates produced.

Figure 2 shows the representative XRD patterns of the calcium phosphate precipitates produced at 120 °C and 180 °C. The peaks of the XRD patterns are in good agreement with the standard JCPDS database (No. 74-0566) and are readily indexable with the HA, space group $P6_3/m$. No obvious peaks other than those due to HA were observed, implying that the impurity is none or in a small amount. Here, it should be mentioned that there has been some recent controversy as to the correct space group of HA [27]. The intensity of the XRD peaks, especially the 100, 101, and 211 peaks, for the 180 °C sample was much stronger than that for the 120 °C sample, which indicated that the precipitates produced at 180 °C were better crystallized than that at 120 °C.

The crystal structure of the as-produced calcium phosphate precipitates was further studied by HRTEM. It confirmed that the dominance of the precipitates produced at 120 °C was of HA structure, but a few OCP crystals were also identified using lattice image and fast Fourier transform (FFT). Figure 3a shows the HRTEM image of the two calcium phosphate precipitate crystals produced at 120 °C. The left crystal was plate-shaped and has well-defined surface contours, whereas the right one was relatively irregular. The FFTs shown in Fig. 3b and c corresponded, respectively, to the left and right crystals shown in Fig. 3a. After carefully measuring the *d*-spacings and interplanar angle from Fig. 3a and b, the left crystal was identified as HA with the [110] zone axis. However, the right crystal was identified as OCP with the [110] zone axis because the faint spots in Fig. 3c (indicated by arrows) implied the ~0.938 nm frequency existing in the right crystal structure. Serious irradiation damage can occur on the as-produced calcium phosphate crystals during high-magnification TEM observation within a few minutes. It was found that the OCP crystals were more readily damaged than the HA crystals under the same dose of electron beam irradiation. This was attributed to the fact that OCP contains ten H_2O molecules in one unit cell.

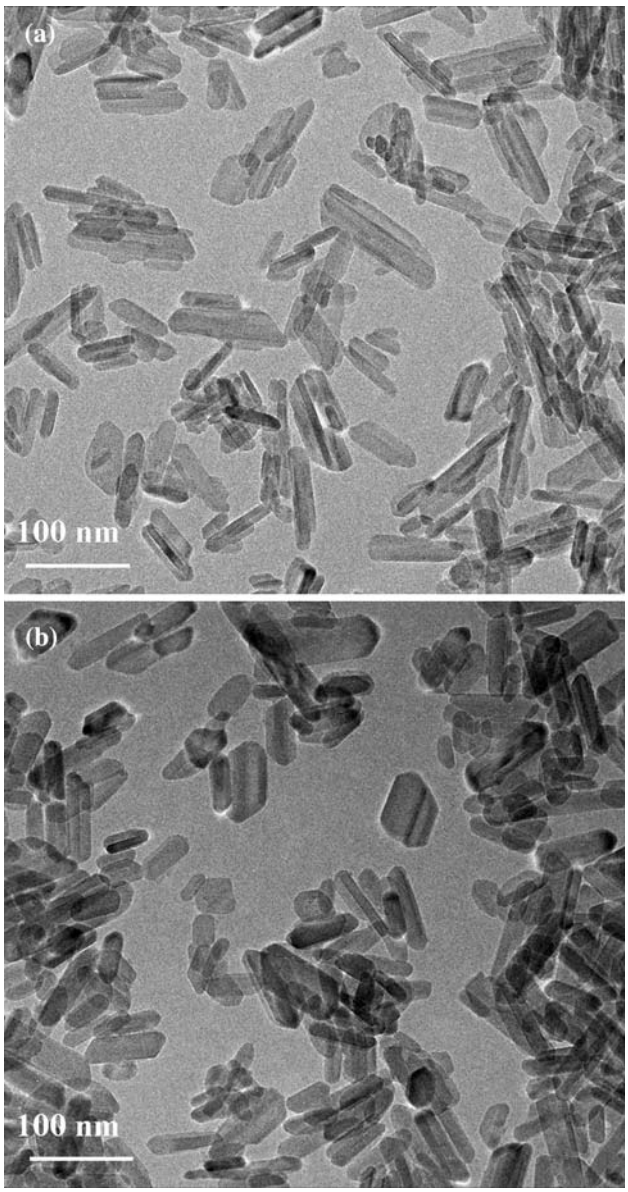

Fig. 1 representative TEM images of the as-produced calcium phosphate nanoparticles by hydrothermal method with the assist of EDTA **a** at 120 °C and **b** at 180 °C

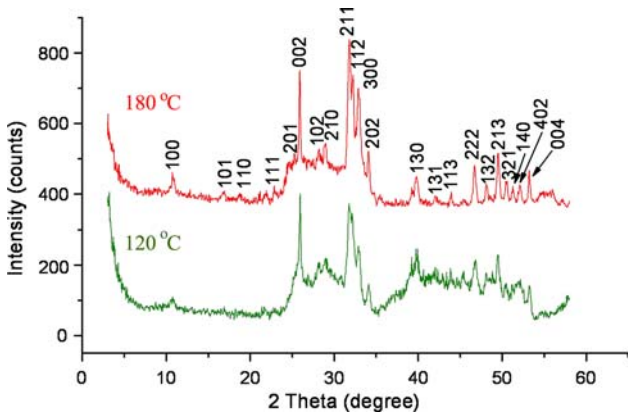

Fig. 2 XRD patterns of the as-produced calcium phosphate nanoparticles

Figure 4a shows the representative HRTEM image of an individual calcium phosphate precipitate produced at 180 °C. The SAED pattern (the inset to Fig. 4a) revealed it was of HA structure with the [110] zone axis and the longitude direction of the HA crystal was along its *c*-axis. It also shows that the apatite precipitates have well-defined surface contours. In order to identify the surface contours of the apatite precipitates, the corresponding FFT of the HRTEM image in Fig. 4a was shown in Fig. 4b. The analyses of the HRTEM image and its FFT indicated that the long and short facets corresponded to HA $(\bar{1}10)$ and $(1\bar{1}\bar{1})$ plane (indicated in Fig. 4a), respectively. The measured interplanar angle of $(\bar{1}10)$ and $(1\bar{1}\bar{1})$ from Fig. 4 is $\sim$131°, which is in good agreement with the computed value of 130.1°. It is worth mentioned that most of the apatite precipitates produced at 180 °C have the same surface contours.

It was commonly believed that OCP was a precursor of apatitic biominerals, and it played an important role in biomineralization [28, 29]. In recent studies, Eliaz et al. observed traces of OCP crystals during the electrocrystallization of HA on titanium at pH 4.2 [30]. We found that OCP was more likely formed on ceramic surfaces than HA in simulated body fluid and we identified OCP structure within HA precipitates in animal body [31, 32]. Here, OCP crystals were confirmed along with HA crystals by HRTEM analyses in the samples produced at 120 °C. This indicated that HA crystals may be formed via an OCP precursor under hydrothermal conditions (pH 9, 120 °C) with the presence of EDTA complex.

Previous studies reported that HA was the only stable calcium phosphate phase at pH >7.4 [21, 30, 33]. The presence of OCP crystals after hydrothermal processing at pH 9 in this study is not contradicted to this point because we found that the solution pH was changed to be 4–5 after hydrothermal processing. Therefore, it might be possible that OCP crystals were formed after the solution became

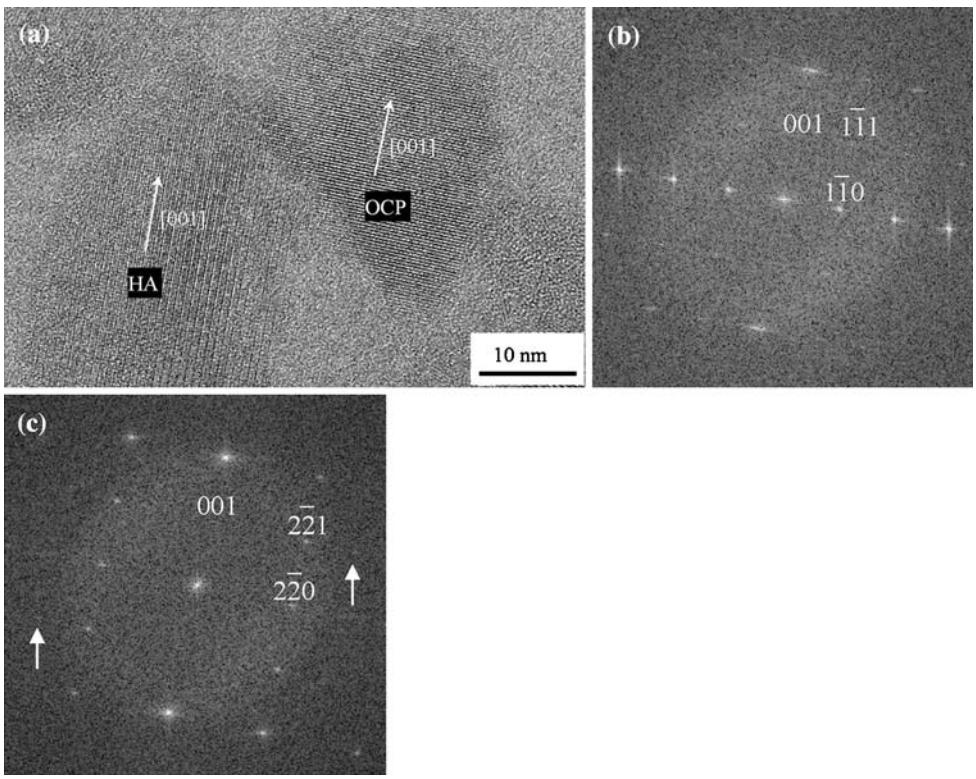

Fig. 3 **a** HRTEM image of the calcium phosphate nanoparticles produced at 120 °C; **b** and **c** are corresponding FFTs of the left and right crystals, respectively, in **a**

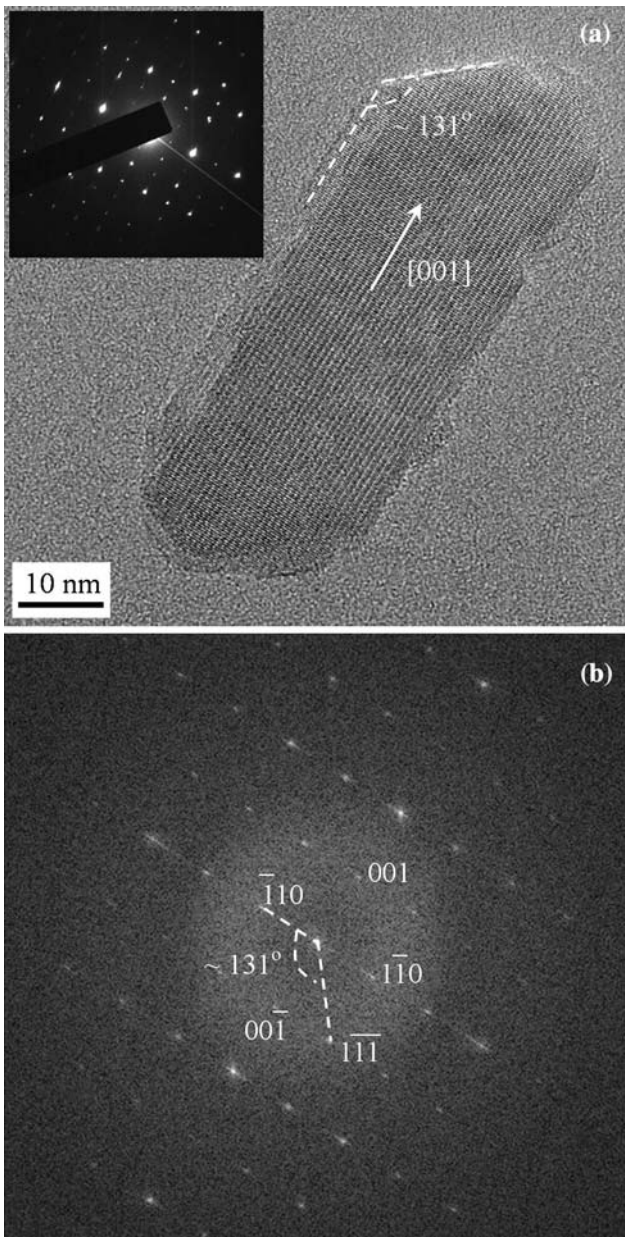

Fig. 4 **a** HRTEM image of the calcium phosphate nanoparticles produced at 180 °C; **b** is the corresponding FFT of **a**

acidic during hydrothermal processing. However, no OCP crystal was detected in the samples produced at 180 °C. This is consistent with Nelson et al.'s finding that the solid-state phase transformation from OCP to HA occurred by heating OCP crystals up to 150 °C [34].

Conclusions

In this article, we synthesized plate-shaped calcium phosphate nanoparticles with length in the range of 50–150 nm by hydrothermal method with EDTA at pH 9. The nanoparticles produced at 180 °C were of HA which was homogenous in structure and shape. However, OCP crystals were detected along with HA crystals in the samples produced at 120 °C. The OCP crystals had less irregular shape and were more electron beam susceptible in TEM than the HA crystals.

Acknowledgement This project was financially supported by National Natural Science Foundation of China (no. 50802119) and supported by Natural Science Foundation Project of CQ CSTC, 2008BB4058.

References

1. Raynaud S, Champion E, Bernache-Assollant D (2002) Biomaterials 23:1073
2. Raynaud S, Champion E, Bernache-Assollant D, Thomas P (2002) Biomaterials 23:1065
3. Rey C, Combes C, Drouet C, Sfihi H, Barroug A (2007) Mat Sci Eng C-Bio S 27:198
4. He QJ, Huang ZL (2007) Cryst Res Technol 42:460
5. Tao JH, Jiang WG, Pan HH, Xu XR, Tang RK (2007) J Cryst Growth 308:151
6. Ye W, Wang XX (2007) Mater Lett 61:4062
7. Zhang X, Vecchio KS (2007) J Cryst Growth 308:133
8. Neira IS, Guitian F, Taniguchi T, Watanabe T, Yoshimura M (2008) J Mater Sci 43:2171. doi:10.1007/s10853-007-2032-9
9. Viswanath B, Ravishankar N (2008) Biomaterials 29:4855
10. Zhang YJ, Lu JJ (2008) Nanotechnology 19
11. Tkalcec E, Sauer M, Nonninger R, Schmidt H (2001) J Mater Sci 36:5253. doi:10.1023/A:1012462332440
12. Montero ML, Sáenz A, Castaño VM (2004) J Mater Sci 39:339. doi:10.1023/B:JMSC.0000007770.88879.76
13. Zhang HB, Zhou KC, Li ZY, Huang SP (2009) J Phys Chem Solids 70:243
14. Liu JB, Li KW, Wang H, Zhu MK, Xu HY, Yan H (2005) Nanotechnology 16:82
15. Chen HF, Sun K, Tang ZY et al (2006) Cryst Growth Des 6:1504
16. Han JK, Song HY, Saito F, Lee BT (2006) Mater Chem Phys 99:235
17. Ashok M, Kalkura SN, Sundaram NM, Arivuoli D (2007) J Mater Sci Mater Med 18:895
18. Li CF, Meng FT (2008) Mater Lett 62:932
19. Singh S, Bhardwaj P, Singh V, Aggarwal S, Mandal UK (2008) J Colloid Interface Sci 319:322
20. Jillavenkatesa A, Hoelzer DT, Condrate RA (1999) J Mater Sci 34:4821. doi:10.1023/A:1004607709747
21. Zhang JM, Tian ZW (1998) J Mater Sci Lett 17:1077
22. Musaev OR, Dusevich V, Wieliczka DM, Wrobel JM, Kruger MB (2008) J Appl Phys 104:084315
23. Zhang Q, Leng Y, Xin R, Wang C, Lu X, Chen J (2007) J Mater Sci 42:6205. doi:10.1007/s10853-006-1121-5
24. Rameshbabu N, Rao KP, Kumar TSS (2005) J Mater Sci 40:6319. doi:10.1007/s10853-005-2957-9
25. Ghaith ES, Hayakawa T, Kasuga T, Nogami M (2006) J Mater Sci 41:2521. doi:10.1007/s10853-006-5241-8
26. Aizawa M, Porter AE, Best SM, Bonfield W (2005) Biomaterials 26:3427
27. Haverty D, Tofail SAM, Stanton KT, McMonagle JB (2005) Phys Rev B 71
28. Brown WE, Eidelman N, Tomazic B (1987) Adv Dent Res 1:306
29. Johnsson MSA, Nancollas GH (1992) Crit Rev Oral Biol M 3:61

30. Eliaz N, Sridhar TM (2008) Cryst Growth Des n 8:3965
31. Xin R, Leng Y, Wang N (2008) Mat Si Eng C-Bio S 28:1255
32. Xin R, Leng Y, Chen J, Zhang Q (2005) Biomaterials 26:6477
33. Redepenning J, Schlessinger T, Burnham S, Lippiello L, Miyano J (1996) J Biomed Mater Res 30:287
34. Nelson DGA, McLean JD (1984) Calcif Tissue Int 36:219